Hydrogen bonding in solid ammonia from *ab initio* calculations

A. D. Fortes,[a] J. P. Brodholt, I. G. Wood, and L. Vočadlo
Research School of Geological and Geophysical Sciences, Birkbeck College and University College London, Gower Street, London WC1E 6BT, United Kingdom

(Received 19 September 2002; accepted 3 January 2003)

We have carried out *ab initio* simulations on the ambient pressure phase I of solid ammonia, and on the high-pressure phase IV. Our plane-wave pseudopotential calculations yield very good agreement with existing structural data, lattice energies, and equations of state. We have also studied the tendency toward symmetrization of the hydrogen bonds at high pressures and find that, unlike pure ice, this process should not occur at experimentally achievable pressures, i.e., <300 GPa. Moreover, our results show that ammonia IV does not contain a bifurcated hydrogen bond, as has previously been suggested. © *2003 American Institute of Physics.* [DOI: 10.1063/1.1555630]

I. INTRODUCTION

Glacial ammonia (NH_3) is intermediate in character between the other two isoelectronic hydrides,[1] water (H_2O), which forms strongly hydrogen bonded tetrahedral structures, and methane (CH_4), a quantum cryocrystal that forms close-packed structures. Weak hydrogen bonding between neighboring ammonia molecules results in a pseudo-close-packed arrangement in the solid state.[2] It is therefore of relevance to chemical physics to understand the nature of hydrogen bonding in crystalline ammonia. Moreover, ammonia is a molecule of some cosmic abundance, believed to comprise a significant fraction of Uranus and Neptune,[3] occurring as stoichiometric hydrates in many icy moons of the outer planets,[4] and playing a role in the chemistry of cloud layers on Jupiter and Saturn.[5] We here characterize solid ammonia at 0 K, up to ~500 GPa, using density functional theory (DFT) calculations.

Our aim is to simulate the behavior of the weak hydrogen bonds in ammonia under compression. We assess the veracity of our calculations by comparing other calculated quantities, such as the equation of state and lattice energy, with existing theoretical results and empirical data. We will therefore start by describing our computational method, and subsequently compare our derived structural, elastic, and thermodynamic properties with known values. This will allow us to confidently discuss our results relating to the hydrogen bonding in solid ammonia in the subsequent section.

A. Ammonia phase relations

The cubic unit cell of ammonia I [Fig. 1(a)] contains four orientationally ordered ammonia molecules on symmetry sites C_{3v}.[6] The dipole moments of the ammonia molecules are directed towards the crystallographic [111] directions. Each molecule both accepts and donates three hydrogen bonds, each of which deviates significantly from the almost perfectly linear hydrogen bonds seen in water ice. Since a single lone-pair orbital is being shared between three nearest neighbors, the hydrogen bonding in ammoniacal solids is very weak, and the result is a pseudo-fcc molecular packing normal to [111]. With increasing pressure and temperature, ammonia experiences a series of phase transitions (Fig. 2), first to hexagonal ammonia II[7] and then to 12-coordinated fcc ammonia III.[8] Both ammonia II and III are rotationally disordered. Above 3.8 GPa at room temperature, ammonia III transforms to an ordered orthorhombic solid, ammonia IV, which crystallizes in space group $P2_12_12_1$.[9] This phase is stable over a wide range of temperatures and pressures. Ammonia IV exhibits pseudo-hcp packing in layers normal to [001] and a more distorted hydrogen bond geometry than in phase I [Fig. 1(b)].

X-ray[2,10–13] and neutron diffraction[6,9,14,15] studies have yielded cell-volume data for solid ammonia from 2–300 K in temperature, and up to 56 GPa in pressure. Structure refinements are available for the ambient pressure phase I up to 0.51 GPa.[7]

B. Previous computational studies

Ab initio methods have been applied to the simulation of ammonia clusters.[16] Our work, however, represents the first time that the plane-wave pseudopotential method has been applied to crystalline ammonia I.

Ammonia IV was the subject of a detailed *ab initio* molecular dynamics study, using density functional theory, at pressures up to 300 GPa, and temperatures up to 7000 K, by Cavazzoni.[17] This study used the Becke[18] exchange functional combined with the Lee, Yang, and Parr[19] correlation functional (collectively BLYP), a particularly popular semi-empirical approach to gradient corrections in quantum chemistry, which has been used successfully on other hydrogen bonded solids.[20] However, the LYP functional violates the requirement that a correlation functional should preserve the correct features of the local spin-density approximation (LSDA) even when there are no regions of small density gradient.[21] The locally based (i.e., nonempirical) Perdew–Wang gradient corrected functional (PW91),[22] which we use here, does not violate this requirement. See Tsuzuki and Lüthi[20] for a quantitative comparison of the performance of the two functionals. The details of our own computational efforts to study ammonia I and IV are presented in the following section.

[a]Electronic mail: andrew.fortes@ucl.ac.uk

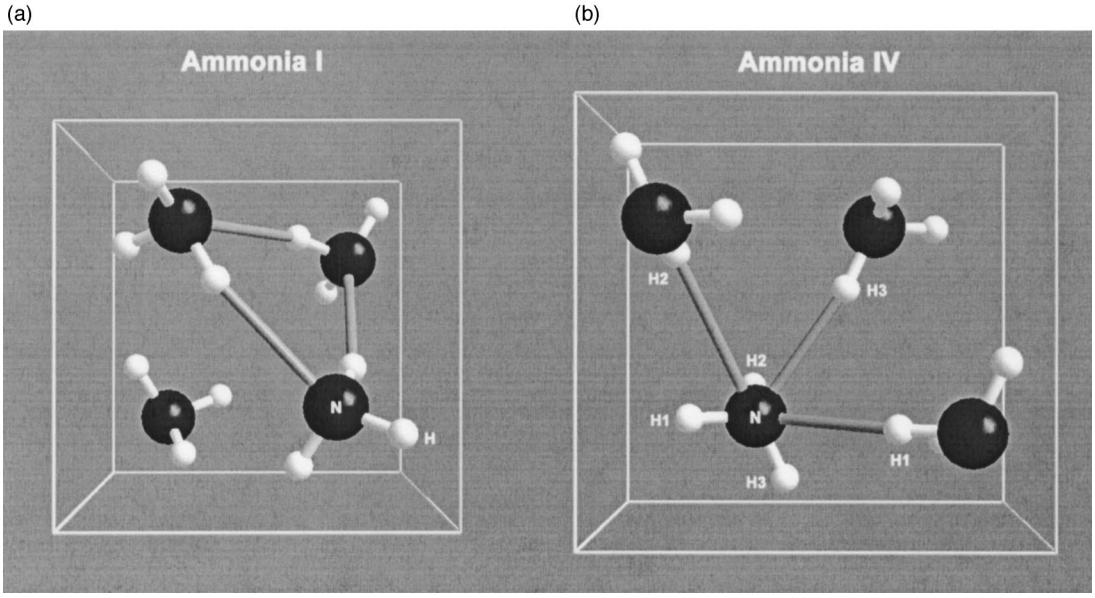

FIG. 1. (a) (left) and (b) (right) The structures of ammonia I and IV, respectively.

II. COMPUTATIONAL METHODS

The plane-wave pseudopotential method, based on density functional theory,[23] was used for calculating the total energy of the crystal lattice. The Perdew–Wang generalized gradient corrected functional (PW91) was applied to represent the exchange-correlation potential,[22] this form of the generalized gradient approximation (GGA) having been demonstrated to yield the most accurate results in hydrogen-bonded systems[20,24] despite not correctly representing dispersion forces. Core electrons are replaced by Vanderbilt nonnormconserving ultrasoft pseudopotentials,[25] themselves formulated within the GGA, and the valence electron wave functions are expanded as a plane-wave basis set. Total energy calculations were performed using the VASP (Vienna *Ab Initio* Simulation Package) code.[26] Convergence tests were carried out to optimize the sampling of the Brillouin zone, and the cutoff of the plane-wave basis set: The Monkhorst–Pack scheme[27] was used for sampling of the Brillouin zone. It was found that for ammonia I (IV) a grid with 32 (27) symmetrically unique $\vec{k}$ points in the irreducible wedge, combined with a kinetic energy cutoff of 900 (1200) eV, yielded total energy convergence to better than 10^{-4} eV per unit cell. A series of fixed volume calculations were then

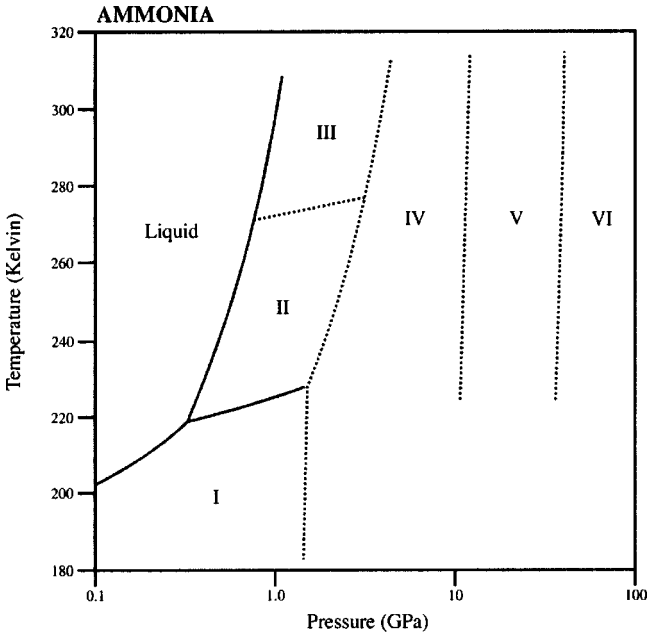

FIG. 2. Phase diagram of solid ammonia, redrawn after Ref. 48. Note that phases V and VI are speculative at present.

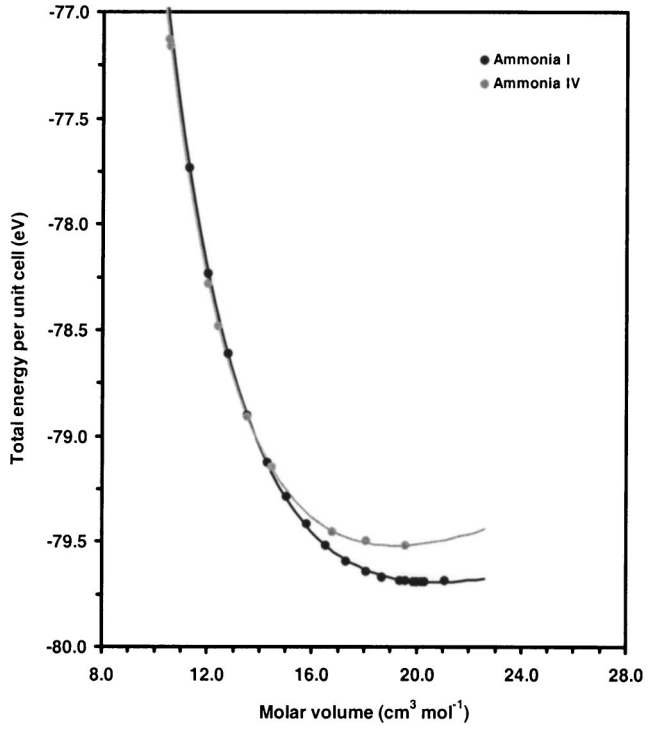

FIG. 3. Calculated total energy as function of molar volume for ammonia I and IV.

TABLE I. Calculated and experimental equation of state parameters of ammonia I.

	V_0 ($cm^3\,mol^{-1}$)	K_0 (GPa)	K_0'	K_0'' (GPa^{-1})	E_0 (eV molecule^{-1})
BMEOS3: $E(V)$	20.65(27)	6.67(70)	5.02(18)		−19.9236(18)
BMEOS3: $P(V)$	20.48(16)	6.53(35)	5.21(9)		
LNEOS4: $E(V)$	20.52(13)	6.94(39)	5.50(3)	−1.65(14)	−19.9239(7)
LNEOS4: $P(V)$	20.50(22)	6.45(56)	5.20(10)	−0.005(3)	
Experimental[a]	19.365	5.8(6)			

[a]Molar volume at 2 K (Ref. 6). Average bulk modulus at ~195 K (see text).

performed in which the ions were allowed to move according to the calculated Hellman–Feynman forces. For each volume specified the structure was relaxed via the conjugate–gradient technique in order to optimize the lattice parameters and internal coordinates.

As a test of the reliability of the supplied pseudopotentials we calculated the relaxed geometry of an isolated ammonia molecule. We found the N–H bond length, $r_{(N-H)} = 1.022$ Å, and the bond angle H–N̂–H = 107.29°. These are a good match to the experimental values, 1.011 Å and 106.80°.[28]

In the following section we report the results of structural relaxations for ammonia I, which were started from the 2 K experimental structure of Hewat and Riekel,[6] and for ammonia IV, which were started from the 5 GPa experimental structure of Loveday *et al.*[9]

III. RESULTS

A. Equation of state

Calculations were performed on the ammonia I structure at unit cell volumes from 27 Å^3 (4.06 $cm^3\,mol^{-1}$) to 170 Å^3 (25.59 $cm^3\,mol^{-1}$), and ammonia IV from 35 Å^3 (5.27 $cm^3\,mol^{-1}$) to 130 Å^3 (19.57 $cm^3\,mol^{-1}$). The plot of total energy against volume, $E(V)$, for both phases is shown in Fig. 3. Integrated forms of the Birch–Murnaghan third order EOS (BMEOS3),[29] and the fourth order logarithmic EOS (LNEOS4),[30] were fitted to the $E(V)$ data. The resulting parameters are given in Tables I and II. Also shown for comparison in Table II are the results of a fit to the combined data sets of Olinger and Mills[12] and Otto *et al.*[13] for ammonia IV. The two EOS were also fitted to the stresses output by VASP at each cell volume, and these parameters are quoted in Tables I and II as well. The fit to the $P(V)$ results is expected to yield more accurate values of higher order derivatives of the pressure with respect to volume, since parameters such as K_0' are second derivatives of pressure, but third derivatives of the energy. Figures 4 and 5 offer a graphical comparison between the calculated EOS and experimental pressure–volume, $P(V)$, data. Note that the EOS of Otto *et al.*[13] is based on an incorrect indexing of the diffraction pattern. However, the error resulting from this is likely to be smaller than the error bars depicted.

The $E(V)$ curves of ammonia I and IV are very flat around V_0, which makes the accurate fitting of an EOS rather difficult. In ammonia I, the GGA appears to overcompensate slightly for the excessive binding seen in typical LDA calculations,[31] resulting in an inflated unit cell. The calculated zero pressure, zero temperature molar volume for ammonia I is ~20.5 $cm^3\,mol^{-1}$, compared with an experimental value of 19.365 $cm^3\,mol^{-1}$ at 2 K,[6] a difference of +5.9%. Hence our ammonia I EOS makes a modest overestimate of the pressure for a given volume, though bearing in mind the relative softness of the bulk modulus, this value is not as problematic as it at first appears. Indeed a pressure of ~3.6 kbar brings the calculated and theoretical volumes into coincidence. The bulk modulus, $K_0 \approx 6.6$ GPa, bears comparison with that found from experimental elastic stiffness coefficients[32,33] and ultrasonic velocity measurements[34] at very much higher temperatures (~195 K).

From the energy of the isolated ammonia monomer (−19.560 eV), the lattice energy of ammonia I is found to be 35.09(17) $kJ\,mol^{-1}$ and the average hydrogen bond enthalpy is 11.90(8) $kJ\,mol^{-1}$. Empirical and theoretical values of the lattice energy are compared in Table III.

At zero pressure, the difference between the calculated

TABLE II. Calculated and experimental equation of state parameters of ammonia IV.

	V_0 ($cm^3\,mol^{-1}$)	K_0 (GPa)	K_0'	K_0'' (GPa^{-1})	E_0 (eV molecule^{-1})
BMEOS3: $E(V)$	19.18(11)	8.71(37)	5.11(7)		−19.8799(10)
BMEOS3: $P(V)$	18.93(19)	9.96(59)	4.84(6)		
LNEOS4: $E(V)$	19.26(20)	9.17(125)	3.49(67)	1.29(15)	−19.8800(11)
LNEOS4: $P(V)$	19.23(27)	9.39(132)	3.26(55)	1.34(22)	
Experiment[a]	19.94(4)	7.56(6)	5.29(3)		
Experiment[b]	18.98(45)	10.11(176)	4.97(26)		

[a]Parameters quoted by Otto *et al.* (Ref. 13).
[b]Our BMEOS3 fit to the experimental density values of Otto *et al.* (Ref. 13) (~210 K) and Olinger and Mills' unpublished x-ray work (Ref. 12) (175–296 K).

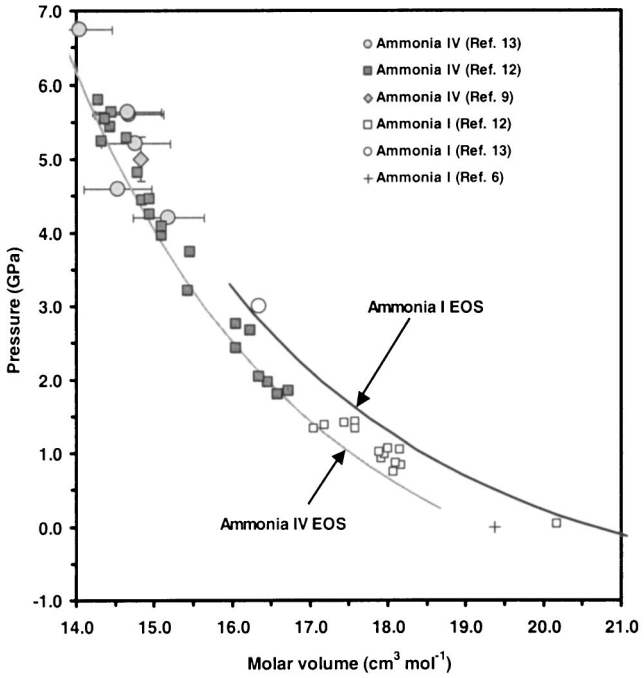

FIG. 4. Low pressure experimental $P(V)$ data for ammonia I and IV, and our calculated equations of state. The large difference in the experimental volumes of ammonia I at zero pressure (cross, Ref. 6; open square, Ref. 12) are due to the large temperature difference (195 K).

V_0 of ammonia IV and the combined fit to the experimental data is within the errors. Figures 4 and 5 show that our EOS falls within all of the error bars of Otto *et al.*[13] For clarity, error bars on Olinger and Mills' unpublished data[12] are not shown but are of the order of 1% in volume.

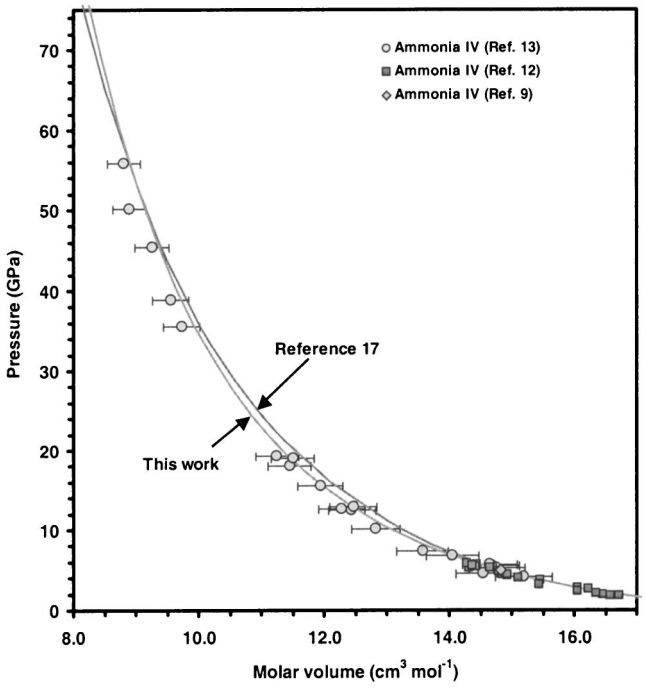

FIG. 5. High pressure experimental $P(V)$ data for ammonia IV, and our calculated EOS.

TABLE III. Experimental and calculated lattice energy of ammonia I.

	Lattice energy ($kJ\,mol^{-1}$)
Experiment (Shipman *et al.*) (Ref. 36)	−36.32(8)
Potential model (Shipman *et al.*) (Ref. 37)	−36.40
Potential model (Hellens) (Ref. 38)	−33.97
Potential model (Snir *et al.*) (Ref. 39)	−37.91
Potential model (Brink and Glasser) (Ref. 40)	−34.23
This work	−35.09(17)

The lattice energy of ammonia IV is found to be $-30.89(11)$ $kJ\,mol^{-1}$ at 0 GPa. The similarity in the lattice energies of ammonia I and IV reflect the similarity in their structures and bonding, which differ only in the second nearest neighbor.

The pressure at which the calculated enthalpies of ammonia I and IV are equal (and hence the phase transition occurs) is 7.5 ± 0.3 GPa. The Raman study of Kume *et al.*[35] indicates that the I–IV transition at 20 K is at ~3 GPa. However, the calculated energy difference between the two phases is so small that the transition pressure is very sensitive indeed to even small errors in the fitted EOS.

B. Structure and bonding

The detailed structural parameters of ammonia I and IV at fixed pressure are presented in Tables IV and V, respectively. So as to compare like for like, experimental and theoretical results are given at the same molar volume.

The structural parameters for ammonia I agree very well with the experimental values.[6] The most significant difference is the overestimate of the N–H bond length, which is carried over from the gas-phase calculation and may be due to inadequacies in the pseudopotentials (see Sec. II). We can confirm that the structure is hydrogen bonded in the expected manner by investigating the electron density along the bond paths between atoms. Interatomic interactions are readily studied in terms of the topological properties of the electron density according to Bader's atoms in molecules theory.[41] Saddle points, or bond critical points, in the charge density (ρ_{bcp} where $\nabla\rho=0$) between atoms have a number of useful properties, not least of which is an estimate of the bond strength.[41] Following Kock and Popelier,[42] we will consider hydrogen bonds as those bonds with $\rho_{bcp}\approx10^{-2}$ a.u. (1 a.u. $=6.7483\,e\,Å^{-3}$) and van der Waals interactions as those with $\rho_{bcp}\approx10^{-3}$ a.u.

We use the VASPViewer program to visualise the electron density in a selected plane which contains the bond under consideration. While this does not allow us to make detailed calculations of quantities such as the Laplacian of the electron density, it does allow the manual location of bond critical points, and the study of electron density along bond paths. For ammonia I, we find that, at the H···N bond critical point, $\rho_{bcp}=0.0137$ a.u., which meets the criterion for a regular hydrogen bond. Electron densities in the plane of the hydrogen bonds are shown for ammonia I and ammonia IV in Figs. 6(a) and 6(b).

TABLE IV. The experimental and calculated structures of ammonia I compared at the same molar volume.

		Experimental values[a]			Calculated values[b]	
	a (Å)	5.048			5.048	
	V (Å^3)	128.63			128.63	
		Fractional atomic coordinates				
	x	y	z	x	y	z
N	0.2109(3)	0.2109(3)	0.2109(3)	0.2086	0.2086	0.2086
H	0.3750(3)	0.2712(4)	0.1129(3)	0.3724	0.2713	0.1060
		Bond lengths (Å)				
N–H		1.012(2)				1.026
H···N		2.357(2)				2.327
		Bond angles				
H–N̂–H		107.53(19)°				108.31°
N–Ĥ···N		160.00(15)°				161.12°

[a]Reference 6, Ref. 14 (0 GPa, 2 K).
[b]This work (0.359 GPa, 0 K).

We can also compare the electron density at the N–H bond critical point with earlier DFT and Hartree–Fock studies,[43] and with experimental values[11] (Table VI). Wang *et al.*[43] employ a variety of different exchange–correlation functionals (although not PW91), including hybrid functionals. In common with our results, all of their DFT calculations yield N–H bond lengths that are 1–1.5 % too long.

The structural parameters of ammonia IV also agree very well with the experimental values.[9] Once again, there is a systematic overestimate of the N–H bond length. However, an interesting feature of our calculated structure is the similarity in the lengths of N–H1, N–H2, and N–H3 (a spread of 0.006 Å) compared with the structure refinement of Loveday *et al.*[9] wherein there is a spread of 0.034 Å in bond lengths. What is worthy of note is that Loveday *et al.*[9] report no significant worsening in the Rietveld fit to their data when all bond lengths and angles are constrained to be equal. We have observed a similar discrepancy between our results and ex-

TABLE V. The experimental and calculated structures of ammonia IV compared at the same molar volume.

		Experimental values[a]			Calculated values[b]	
	a (Å)	3.2495(4)			3.2476	
	b (Å)	5.6576(6)			5.5977	
	c (Å)	5.3556(5)			5.4155	
	b/a	1.7411(4)			1.7236	
	c/a	1.6481(3)			1.6679	
	V (Å^3)	98.45(3)			98.45	
		Fractional atomic coordinates				
	x	y	z	x	y	z
N	0.2604(11)	0.3509(4)	0.2563(5)	0.2640	0.3574	0.2543
H1	0.3795(16)	0.1918(9)	0.2352(11)	0.3816	0.1885	0.2318
H2	−0.0294(23)	0.3340(9)	0.3240(12)	−0.0273	0.3382	0.3232
H3	0.2312(24)	0.4238(7)	0.0902(12)	0.2281	0.4290	0.0805
		Bond lengths (Å)				
N–H1		0.980(6)				1.027
N–H2		1.014(8)				1.023
N–H3		0.985(7)				1.029
H1···N		2.257(6)				2.183
H2···N′		2.338(8)				2.334
H2···N″		2.572(7)				2.629
H3···N		2.196(6)				2.133
		Bond angles				
H1–N̂–H2		106.3(5)°				106.87°
H1–N̂–H3		115.0(4)°				107.01°
H2–N̂–H3		105.8(6)°				105.67°
N–Ĥ···N		171.86(45)°				166.82°
N–Ĥ2···N′		149.06(63)°				148.08°
N–Ĥ···N″		126.71(51)°				126.94°
N–Ĥ3···N		167.71(48)°				166.87°

[a]Reference 9 (5 GPa, $T=150$ K).
[b]This work (4.327 GPa, 0 K).

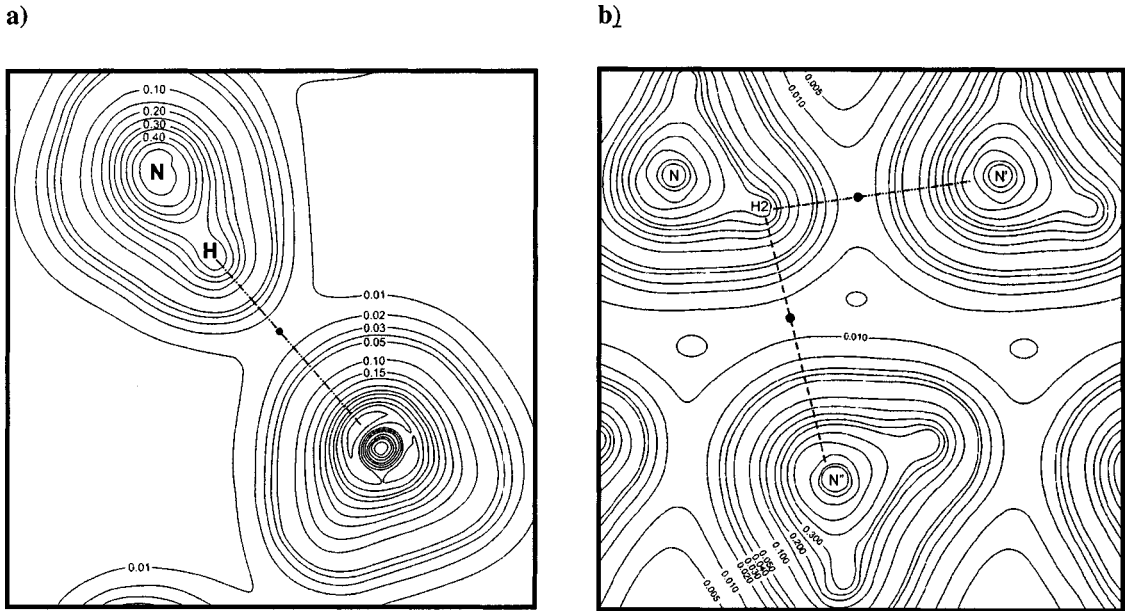

FIG. 6. (a) Electron density in ammonia I in the plane of the hydrogen bond. Contours are in intervals of 0.01 a.u. up to 0.05 a.u., and in intervals of 0.05 a.u. thereafter. The bonding path is denoted by the dotted–dashed line, and bond critical point of the hydrogen bond by the filled circle. (b) Electron density in ammonia IV in the plane of the proposed bifurcated hydrogen bond. Contours are as in (a) except for the contour at 0.005 a.u. The bonding paths are denoted by the dotted–dashed and dashed lines, and the bond critical points by the filled circles.

perimental structure refinements for N–H bond lengths in ammonia monohydrate phase I[44] and ammonia dihydrate phase I.[45]

Figure 7 depicts the calculated cell parameters of ammonia IV as a function of molar volume. These results are compared with the DFT result of Cavazzoni at 300 K,[17] and the experimental neutron diffraction[9] and x-ray data.[13] The x-ray data was indexed on the basis of a hexagonal unit cell (hence giving only a and c), so we have calculated the length of the b axis, for comparison purposes only, on the assumption of an ideal hcp b/a ratio$=\sqrt{3}a$. It is apparent that the agreement with experimental data is poorer at low pressures but improves under compression.

As mentioned previously, the structure of ammonia IV is of particular note because of the possibility that it might contain a bifurcated hydrogen bond[9] (strictly, a three-centered interaction: A three-centered hydrogen bond describes the situation where a hydrogen atom is surrounded by three electronegative atoms lying approximately in a plane containing the hydrogen atom, and where the hydrogen atom is covalently bound to one of the three surrounding atoms). Bifurcated hydrogen bonds play a very important role in, for example, the structure and stability of biological molecules such as DNA,[46] and the occurrence of such a bond in as simple a material as glacial ammonia would be of great potential interest. Loveday *et al.*[9] proposed the aforementioned bifurcated bond on the grounds of the strained character of the N–$\hat{\text{H}}$2$\cdots$N′ bond angle (149° compared with ~170° for the other N–$\hat{\text{H}}\cdots$N angles) and the observation that the H2$\cdots$N″ distance is slightly less than the sum of the van der Waals radii for deuterium and nitrogen (2.75 Å). The geometry of the proposed bifurcated hydrogen bond is strikingly similar to structure-type **II4** examined by Rozas *et al.*[47] in their computational study of three-centered interactions. Their example of a proposed asymmetric three-center interaction failed to reveal a second hydrogen bond (on the basis

TABLE VI. Electron densities at the N–H bond critical point.

	Experiment[a]	MP2/6-31G(3d)[b]	DFT[c]	This work
ρ_{bcp} (a.u.)	0.317(6)	0.332	0.327–0.336	0.314
$r_{(\text{N–H})}$ (Å)	1.010	1.020	1.019–1.028	1.026
$r_{(\text{bcp–H})}$ (Å)	0.245	0.246	0.242–0.253	0.245

[a]Electron diffraction at 160 K (Ref. 11).
[b]Reference 43.
[c]Density functional calculations with various gradient approximations (Ref. 43).

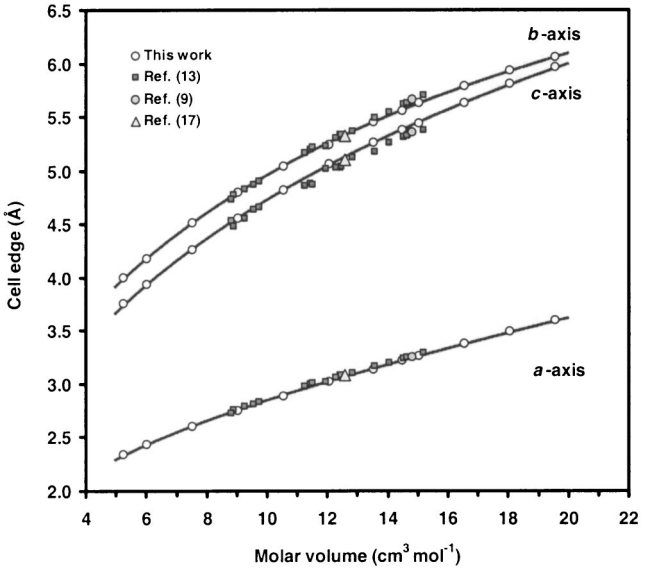

FIG. 7. Volume dependence of the cell parameters in ammonia IV.

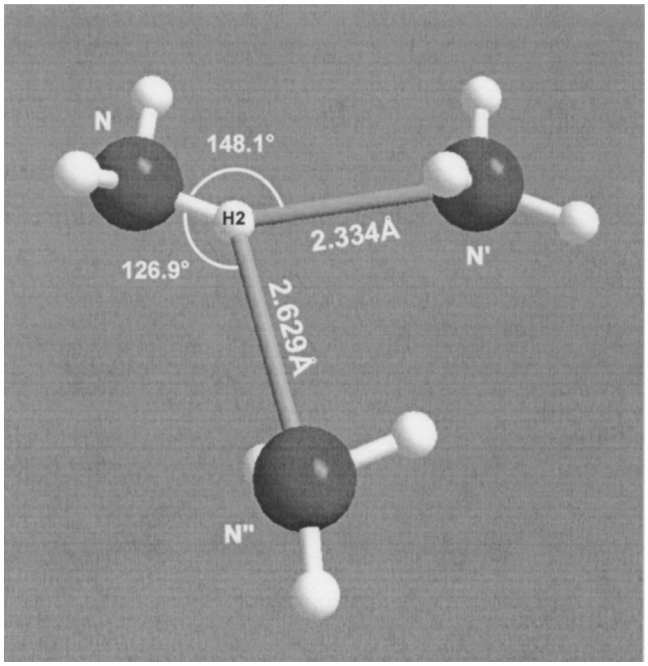

FIG. 8. The geometry of the proposed bifurcated hydrogen bond in ammonia IV. This view corresponds approximately to that depicted in Fig. 6(b). Bond lengths and angles are as Table V.

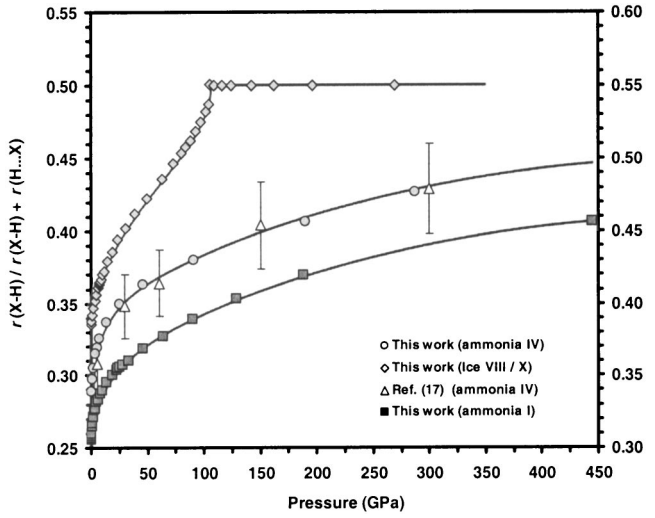

FIG. 9. Variation of the fractional hydrogen bond length, $r_{(X-H)}/r_{(X-H)}+r_{(H\cdots X)}$, where X=O or N, in ice and ammonia, respectively. The ice VIII data shows a continuous trend towards symmetrical hydrogen bonds at ~105 GPa, though this process is in fact interrupted by a phase transition to a bond-symmetrized phase at ~70 GPa. Note that the data for ammonia I should be read from the right-hand axis; that for ice VIII/X and ammonia IV from the left-hand axis.

of ρ_{bcp}) which would be the equivalent of H2···N″ in the ammonia IV structure. Instead it was concluded that this geometry corresponds to a single strong hydrogen bond perturbed by van der Waals forces from a nearby interacting atom. It is therefore intriguing to examine the electron density in our calculated ammonia IV structure so as to shed light on the existence, or otherwise, of a bifurcated hydrogen bond.

Our simulated structure confirms the presence of this strained bond, and also reveals that it is present at all pressures studied (up to ~500 GPa). Bond critical points are present in the charge density topology of ammonia for the three expected hydrogen bonds, H1···N ($\rho_{bcp}=0.0196$ a.u.), H2···N′ ($\rho_{bcp}=0.0150$ a.u.), and H3···N ($\rho_{bcp}=0.0250$ a.u.), and the bond strength indicated by these values (at 5 GPa) agrees with the order inferred from inspecting the bond lengths (Table V). In other words, the hydrogen bond strength, E_{HB}, follows the pattern (H3···N)>(H1···N)>(H2···N′). As Fig. 6(b) shows, the electron density along the proposed H2···N″ bond path (dashed line) is very small, ~0.0074 a.u. at the saddle point, which indicates no hydrogen bond. This value is no higher than the electron density between other *nonbonded* nitrogen and hydrogen atoms. We therefore conclude that this bond geometry in ammonia IV is entirely analogous to that in structure-type **II4** of Rozas *et al.*,[47] in which a single hydrogen bond is perturbed by a neighboring atom: Ammonia IV does not contain a bifurcated hydrogen bond. (See Fig. 8.)

C. Hydrogen-bond symmetrization

In ice the hydrogen bond is pressure strengthened, leading to an increase of the covalent O–H bond length, $r_{(O-H)}$, up to the limit in which the proton is symmetrically located midway between neighboring oxygen atoms, producing the Cu_2O structured ice X. A similar phenomenon has been proposed for ammonia on the basis of Raman observations. Two possible high-pressure (>60 GPa) structures were mooted:[48] The first is isostructural with Cu_3N (space group $Pm3m$ O_h^1) with H–N̂–H angles of 90°. The second proposed structure has space group $Pn3m$ (O_h^4), and H–N̂–H bond angles of 141°. An x-ray study up to 56 GPa[13] failed to observe the proposed precursor[48] to these structures (ammonia V: space group $I\bar{4}3m$), and more recent infrared spectroscopy has ruled out bond symmetrization up to 120 GPa.[49] Moreover, Cavazzoni[17] did not see bond symmetrization at pressures up to 300 GPa, and found that the proposed cubic structure was energetically disfavored with respect to ammonia IV.

We have studied the behavior of the hydrogen bonds under compression up to ~300 GPa in both ammonia I and ammonia IV. The results are shown in Fig. 9, alongside Cavazzoni's results[17] and our calculations for the ice VIII/X transition quoted as $r_{(X-H)}/[r_{(X-H)}+r_{(H\cdots X)}]$, where X=O in ice and N in ammonia. Observe that the data for ammonia I is downshifted for ease of viewing, and values should be read from the axis on the right. The data for ammonia IV consists of an average of the three N–H bond lengths. Similarly, Cavazzoni plots the abscissa of the peak in the radial distribution function (effectively an average of the three N–H bond lengths).[17] In ice VIII, we observed in our calculations that the fractional hydrogen bond length and the degree of tetragonal distortion from the cubic ice X structure behaved as coupled order parameters, tending continuously to a cubic symmetrized phase near 100 GPa. However, the ice X structure was found to be thermodynamically stable at much lower pressures, as determined from the separately calculated EOS of each phase, and we place the transition at 70(1) GPa. This pressure is in agreement with experimental

values. This apparent contradiction in the phase transition pressures (between the case where ice VIII and ice X are simulated separately, and the case where ice VIII is compressed until it becomes ice X) occurs because our calculations treat the hydrogen atom as a classical entity (subject to Newtonian mechanics) rather than as a quantum entity. Since this overlooks the important delocalizing effects of tunnelling and zero-point motion,[50] the transition pressure (under continuous compression of the ice VIII structure) is pushed to 100 GPa, rather than 70 GPa.

Within the stability field of ammonia I, the N–H bonds behave in the same way as the O–H bonds in ice VIII, increasing in length at a rate of 0.038(1) pm GPa^{-1} up to 4 GPa. Beyond that pressure, in phases I and IV, the N–H bonds decrease in absolute length but continue to increase in fractional length $(r_{(X-H)}/[r_{(X-H)}+r_{(H\cdots X)}])$, trending towards the symmetrical limit. Nonetheless, this limit is not reached up to the highest pressure we investigated.

Our overall finding is that hydrogen bond symmetrization should not occur in ammonia IV at any experimentally reasonable pressure (i.e., <300 GPa). Indeed, extrapolating our results to $r_{(X-H)}/[r_{(X-H)}+r_{(H\cdots X)}]=\frac{1}{2}$ suggests a symmetrization pressure well in excess of 2 TPa. This is not to say that ammonia IV does not transform via a first order process to some other structure in which symmetrical hydrogen bonding is achievable at a much lower pressure. This conclusion also does not include the important quantum effects of tunnelling and zero-point motion, which would act to bring the symmetrisation transition to a lower pressure.

IV. SUMMARY

We have undertaken plane-wave pseudopotential calculations on the ambient-pressure phase of glacial ammonia, and the high-pressure phase, ammonia IV. Our structures, equations of state, and lattice energies for ammonia I are in good agreement with experimental data. Similarly, where there is experimental data for ammonia IV, our calculations also yield very good results. Our results on the pressure dependence of the hydrogen bond strength in ammonia IV are in excellent accord with an earlier DFT study and confirm the latest Raman studies. Moreover, we have shown that ammonia IV does not contain a bifurcated hydrogen bond; rather it contains a hydrogen bond which is perturbed by van der Waals forces. The principle error in our method is the classical treatment of the hydrogen atoms.

ACKNOWLEDGMENTS

One of the authors (A.D.F.) acknowledges a scholarship from the UCL Graduate School in support of this work. L.V. and J.P.B. are supported by the Royal Society. The authors would also like to thank David Price, Stefan Klotz, Vadim Manzhelii, and Carlo Cavazzoni for useful comments and practical assistance.

[1] R. L. DeKock and H. B. Gray, *Chemical Structure and Bonding* (University Science Books, Mill Valley, CA, 1989).
[2] J. W. Reed and P. M. Harris, J. Chem. Phys. **35**, 1730 (1961).
[3] W. B. Hubbard and J. J. McFarlane, J. Geophys. Res. B **85**, 225 (1980).
[4] J. S. Kargel, Icarus **100**, 556 (1992).
[5] P. G. J. Irwin, Surv. Geophys. **20**, 505 (1999).
[6] A. W. Hewat and C. Riekel, Acta Crystallogr., Sect. A: Cryst. Phys., Diffr., Theor. Gen. Crystallogr. **A35**, 569 (1979).
[7] J. Eckert, R. L. Mills, and S. K. Satija, J. Chem. Phys. **81**, 6034 (1983).
[8] R. B. von Dreele, Acta Crystallogr., Sect. C: Cryst. Struct. Commun. **C40**, 1635 (1984).
[9] J. S. Loveday, R. J. Nelmes, W. G. Marshall, J. M. Besson, S. Klotz, and G. Hamel, Phys. Rev. Lett. **76**, 74 (1996).
[10] I. Olovsson and D. H. Templeton, Acta Crystallogr. **12**, 832 (1959).
[11] R. Boese, N. Niederprijm, D. Blaser, A. Maulitz, M. Y. Antipin, and P. R. Mallinson, J. Phys. Chem. B **101**, 5794 (1997).
[12] B. Olinger and R. L. Mills (unpublished).
[13] J. W. Otto, R. F. Porter, and A. L. Ruoff, J. Phys. Chem. Solids **50**, 171 (1989).
[14] F. Leclerq, P. Damay, and M. Foukani, J. Chem. Phys. **102**, 4400 (1995).
[15] J. S. Loveday, G. Hamel, R. J. Nelmes, S. Klotz, M. Guthrie, and J. M. Besson, High Press. Res. **17**, 149 (2000).
[16] W. Koch and M. C. Holthausen, *A Chemist's Guide to Density Functional Theory*, 2nd ed. (Wiley-VCH, Verlag GmbH, Weinheim, Germany, 2001).
[17] C. Cavazzoni. Ph.D. thesis, International School for Advanced Studies (Scuola Internazionale Superiore di Study Avanzati), Trieste, Italy, 1998; C. Cavazzoni, G. L. Chiarotti, S. Scandolo, E. Tosatti, M. Bernasconi, and M. Parrinello, Science **283**, 44 (1999).
[18] A. D. Becke, Phys. Rev. A **38**, 3098 (1988).
[19] C. Lee, W. Yang, and R. G. Parr, Phys. Rev. B **37**, 785 (1988).
[20] S. Tsuzuki and H. P. Lüthi, J. Chem. Phys. **114**, 3949 (2001).
[21] K. Burke, J. P. Perdew, and M. Ernzehof, Int. J. Quantum Chem. **61**, 287 (1997).
[22] J. P. Perdew, in *Electronic Structure of Solids*, edited by P. Zeische and H. Eschrig (Akademie, Berlin, 1991), p. 11; J. P. Perdew and Y. Wang, Phys. Rev. B **45**, 13244 (1992).
[23] P. Hohenberg and W. Kohn, Phys. Rev. **136**, B864 (1964); W. Kohn and L. J. Sham, Phys. Rev. **140**, A1133 (1965).
[24] D. R. Hamann, Phys. Rev. B **55**, 10157 (1997).
[25] D. Vanderbilt, Phys. Rev. B **41**, 7892 (1990).
[26] G. Kresse and J. Furthmüller, Phys. Rev. B **54**, 11169 (1996).
[27] H. J. Monkhorst and J. D. Pack, Phys. Rev. B **13**, 5188 (1976).
[28] J. Demaison, L. Margulès, and J. E. Boggs, Chem. Phys. **260**, 65 (2000).
[29] F. Birch, J. Geophys. Res. **57**, 227 (1952).
[30] J.-P. Poirier and A. Tarantola, Phys. Earth Planet. Inter. **109**, 1 (1998).
[31] J. Hafner, Acta Mater. **48**, 71 (2000).
[32] H. Kiefte, S. W. Breckon, R. Penney, and M. J. Clouter, J. Chem. Phys. **83**, 4738 (1985).
[33] H. Kiefte, R. Penney, S. W. Breckon, and M. J. Clouter, J. Chem. Phys. **86**, 662 (1987).
[34] E. I. Voitovich, A. M. Tolkachev, and V. G. Manzhelii, J. Low Temp. Phys. **5**, 435 (1971).
[35] T. Kume, S. Sasaki, and H. Shimizu, J. Raman Spectrosc. **32**, 383 (2001).
[36] L. L. Shipman, A. W. Burgess, and H. A. Scheraga, J. Phys. Chem. **80**, 52 (1976).
[37] L. L. Shipman, A. W. Burgess, and H. A. Scheraga, Proc. Natl. Acad. Sci. U.S.A. **72**, 543 (1975).
[38] R. L. Hellens, Ph.D. thesis. Yale University, 1951.
[39] J. Snir, R. A. Nemenoff, and H. A. Scheraga, J. Phys. Chem. **82**, 2510 (1978).
[40] G. Brink and L. Glasser, J. Mol. Struct. **160**, 357 (1987).
[41] R. F. W. Bader, *Atoms in Molecules—A Quantum Theory*, International Series of monographs on Chemistry 22 (Oxford University Press, Oxford, 1990).
[42] U. Kock and P. L. A. Popelier, J. Phys. Chem. **99**, 9747 (1995).
[43] J. Wang, B. G. Johnson, R. J. Boyd, and L. A. Eriksson, J. Phys. Chem. **100**, 6317 (1996).
[44] A. D. Fortes, J. P. Brodholt, I. G. Wood, L. Vočadlo, and H. D. B. Jenkins, J. Chem. Phys. **115**, 7006 (2001).
[45] A. D. Fortes, I. G. Wood, J. P. Brodholt, and L. Vočadlo, Icarus (to be published).
[46] D. Bhattacharyya and R. Majumdar, Indian J. Biochem. Biophys. **38**, 16 (2001).
[47] I. Rozas, I. Alkorta, and J. Elguero, J. Phys. Chem. A **102**, 9925 (1998).
[48] M. Gauthier, Ph. Pruzan, J. C. Chervin, and J. M. Besson, Phys. Rev. B **37**, 2102 (1988).
[49] M. Sakashita, H. Yamawaki, H. Fujihisa, and K. Aoki, Rev. High Pressure Sci. Technol. **7**, 796 (1998).
[50] M. Benoit, D. Marx, and M. Parrinello, Nature (London) **392**, 258 (1997).